ELSEVIER

Inorganica Chimica Acta 225 (1994) 1–7

Inorganica Chimica Acta

Effect of substituting sulfur for oxygen on the heterogeneous electron transfer kinetics of oxomolybdenum(V) hydrotris-(3,5-dimethyl-1-pyrazolyl)borate complexes

Gloria M. Olson, Franklin A. Schultz*

Department of Chemistry, Indiana University–Purdue University at Indianapolis, 402 North Blackford Street, Indianapolis, IN 46202-3274, USA

Received 10 January 1994

Abstract

Heterogeneous electron transfer rate constants ($k_{s,h}$) and formal potentials ($E°'$) are measured for the one-electron reduction of a series of oxomolybdenum(V) complexes, $HB(Me_2pz)_3MoO(L\text{-}L)$, where $HB(Me_2pz)_3^-$ = hydrotris(3,5-dimethyl-1-pyrazolyl)borate and $L\text{-}L^{2-}$ is a bidentate 1,2-disubstituted ethane or benzene ligand whose donor atoms can be either O or S. $E°'$ shifts in the negative direction by about 1 V and $k_{s,h}$ decreases by about 1.5 orders of magnitude as S is replaced by O in the inner coordination sphere of these compounds. These observations are rationalized in terms of a hard acid–hard base interaction between the $HB(Me_2pz)_3MoO^{2+}$ fragment and $L\text{-}L^{2-}$ which stabilizes the metal–ligand bond and increases the energy of the metal-centered redox orbital as the hard base character of the bidentate ligand increases. Electron transfer rate differences are believed to arise primarily from larger inner-shell contributions to the activation energy barrier for Mo–O versus Mo–S complexes, but contributions from differences in outer-shell energies and adiabaticities cannot be eliminated at this time.

Keywords: Electron transfer; Kinetics; Molybdenum complexes; Oxo complexes

1. Introduction

A current question in electron transfer chemistry concerns the influence of the inner coordination shell on the kinetics and thermodynamics of metal-centered electron transfer reactions. Marcus–Hush theory [1] predicts that when changes in nuclear coordinates result in large reorganization energies (Franck–Condon factors), thesc barriers can slow the rate of electron transfer. Thus, if 'soft' sulfur donors are replaced by 'hard' oxygen atoms in the coordination shell of a metal, the stronger metal–oxygen bonds will result in more negative reduction potentials and more sluggish electron transfer kinetics. These anticipated consequences of O/S substitution on oxidation-reduction potentials and electron transfer kinetics have been observed qualitatively on a number of occasions [2–7]. Exemplary results are those of Bond et al. [2], who demonstrated that the reductions of metal–thioacetylacetonate derivatives are thermodynamically and kinetically more facile than those of their oxygen containing counterparts, and of Wieghardt and co-workers [7], who rationalized the faster self-exchange kinetics of $Co(ttcn)_2^{3+/2+}$ (ttcn = 1,4,7-trithiacyclononane, $k_{ex} = 1.3 \times 10^4\ M^{-1}\ s^{-1}$) vis-à-vis $Co(tacn)_2^{3+/2+}$ (tacn = 1,4,7-triazacyclononane, $k_{ex} = 0.19\ M^{-1}\ s^{-1}$) on a similar basis. However, systematic investigation of O versus S coordination on the kinetic and thermodynamic properties of a single series of compounds has not been realized.

This paper reports an investigation of the electrochemical reduction kinetics of the oxomolybdenum(V) complexes [8] illustrated in Fig. 1. The compounds contain two equatorial sites at which O donor atoms can be incrementally exchanged for S by varying substituents on the 1,2-disubstituted ligands. The initial description of these compounds [8] reported an unusually large range (>1 V) in their $Mo^{V/IV}$ reduction potentials. Based on the considerations stated above, parallel differences in kinetic behavior are anticipated. The present paper reports measurement of the $Mo^{V/IV}$ heterogeneous electron transfer rates for this series of compounds and correlation of the findings with their molecular structure.

*Corresponding author.

SSDI 0020-1693(94)04022-N

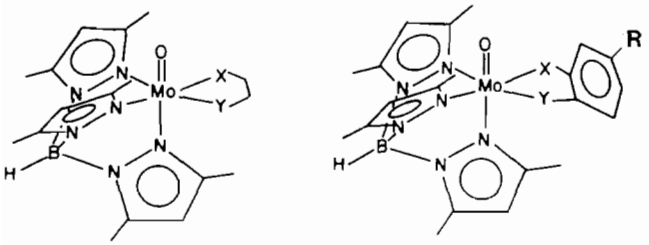

1a	X,Y = O	**2a**	X,Y = O; R = H
1b	X = O, Y = S	**2b**	X = O, Y = S; R = H
1c	X,Y = S	**2c**	X,Y = S; R = CH_3

Fig. 1. Structures of $HB(Me_2pz)_3MoO(L\text{-}L)$ complexes.

2. Experimental

2.1. Materials

The hydrotris(3,5-dimethyl-1-pyrazolyl)borate ($HB(Me_2pz)_3^-$) ligand was isolated as its potassium salt following the procedure of Trofimenko [9]. Compounds **1a–1c** and **2a–2c** (Fig. 1) were prepared from $HB(Me_2pz)_3MoOCl_2$ and the corresponding 1,2-disubstituted ethane or benzene as described by Enemark and co-workers [8a] and characterized by IR and UV–Vis spectroscopy. Purity was established by measurement of molar absorptivities and voltammetric peak current parameters.

Electrochemical experiments were conducted in HPLC grade acetonitrile (Aldrich) which had been freshly distilled from P_2O_5 under N_2. The supporting electrolyte, tetra-n-butylammonium hexafluorophosphate (BuN_4PF_6) from Southwestern Analytical Chemicals, was recrystallized twice from ethanol and dried under vacuum at 80 °C.

2.2. Equipment and procedures

Electrochemical experiments were conducted at Pt disk working electrodes having radii of 50, 125 and 800 μm. The 50 and 800 μm electrodes were purchased from Bioanalytical Systems (West Lafayette, IN). The 125 μm electrode was prepared by sealing Pt wire into soft glass. All electrodes were polished with 0.05 μm alumina (Buehler) and rinsed with distilled water, acetone and acetonitrile before use.

Electrode kinetic measurements were carried out by cyclic voltammetry using a BAS 100A potentiostat at slow scan rates and an EG&G PAR 173 potentiostat driven by a Hewlett Packard 3300A function generator at fast scan rates. The current follower circuit of Fitch and Evans [10] was used in conjunction with the PAR 173 to amplify signals from the smaller electrodes. A Nicolet 4094C digitizing oscilloscope was used as a data collection device in the fast sweep rate experiments. Kinetic measurements with the 800 μm electrode were made with a previously published cell design [11], which afforded 0.5 mm spacing between the working and reference electrodes and the ability to compensate for solution resistance. A conventional electrochemical cell was used for the smaller electrodes. The auxiliary electrode was a Pt wire, and the reference electrode was an aqueous Ag/AgCl half-cell immersed in a salt bridge containing supporting electrolyte and whose potential was determined to be 0.197 V versus NHE by ferrocene calibration [12]. Experiments were conducted at 23 ± 1 °C.

Apparent values of the standard heterogeneous rate constant, $k_{s,h}$, were determined from the scan rate dependence of cyclic voltammetric peak potential separations, ΔE_p, using the method of Nicholson [13]. The electrode size, reactant concentration and scan rate range were chosen to provide $\Delta E_p = 80$–200 mV for each redox couple while minimizing the effects of uncompensated solution resistance and edge diffusion [14]. In practice, this translated into use of scan rate ranges of 0.01–0.5, 1–20 and 10–75 V s^{-1} at the 800, 125 and 50 μm electrodes, respectively. In addition, experimental peak potential separations were corrected for residual *iR* drop and edge diffusion effects by subtraction of the terms $(\Delta E_p)_{iR}$ and $(\Delta E_p)_{edge}$ from $(\Delta E_p)_{meas}$ to obtain $(\Delta E_p)_{kin}$:

$$(\Delta E_p)_{kin} = (\Delta E_p)_{meas} - (\Delta E_p)_{iR} - (\Delta E_p)_{edge} \quad (1)$$

$(\Delta E_p)_{iR}$ accounts for the contributions of both faradaic and capacitive currents to the *iR* drop as calculated from Eq. (2)

$$(\Delta E_p)_{iR} = 2(i_p + i_c)R_u = (\pi/2)\rho r[0.446F^{3/2}(D/RT)^{1/2}C_O\nu^{1/2} + C_{dl}\nu] \quad (2)$$

where D and C_O are the diffusion coefficient and concentration, respectively, of the reactant, ρ is the resistivity of the supporting electrolyte, r is the electrode radius, C_{dl} is the double layer capacitance and ν is the potential scan rate. Values of $(\Delta E_p)_{edge}$ were obtained from the tabulation of Heinze [15]. The sum of corrections to $(\Delta E_p)_{meas}$ was typically 1–2 mV and never exceeded 8 mV. Values of $(\Delta E_p)_{kin}$ obtained from Eq. (1) were used in conjunction with diffusion coefficients determined by chronocoulometry and the value $\alpha = 0.50$ to determine $k_{s,h}$. The reliability of the foregoing procedure was evaluated by measuring the rate constant for ferrocene oxidation in acetonitrile containing 0.3 M BuN_4PF_6 at the 50 μm electrode. A value of

$k_{s,h} = 1.0 \pm 0.2$ cm s^{-1} was obtained in good agreement with recent determinations of this parameter [16].

3. Results and discussion

Fig. 2 illustrates the voltammetric behavior of the $HB(Me_2pz)_3MoO(L\text{-}L)$ complexes. Each compound exhibits a chemically reversible one-electron reduction that is attributed to the following reaction:

$$HB(Me_2pz)_3Mo^{V}O(L\text{-}L) + e^- \rightleftharpoons [HB(Me_2pz)_3Mo^{IV}O(L\text{-}L)]^- \quad (3)$$

In addition, compounds **1a–c**, **2a** and **2b** exhibit an irreversible oxidation at 1.2 to 1.6 V that is not systematically dependent on the identity of L-L. Compound **2c** exhibits a reversible one-electron oxidation at 1.00 V that is assigned to oxidation of the coordinated toluene-3,4-dithiolate ligand. The anodic reactions of these complexes are not considered further. Reaction (3) is established to be a diffusion-limited, chemically reversible, one-electron process by virtue of the linear dependence of its voltammetric peak current (i_p) on the square rate of scan rate (ν), a reverse-to-forward peak ratio (i_{pr}/i_{pf}) of approximately unity and a voltammetric peak current parameter ($i_p/\nu^{1/2}$a.c.), which is nearly equal to that of other one-electron reactants in CH_3CN [17]. Electrochemical data for reaction (3) are collected in Table 1.

The formal potential of $Mo^{V/IV}$ reduction varies between −0.1 and −1.14 V versus Ag/AgCl and increases systematically in the negative direction as each S donor atom is replaced by oxygen in the 1,2-disubstituted ethanes and benzenes. The shift in $E^{\circ\prime}$ is approximately 0.3 V per atom in the aromatic and 0.4 V per atom in the saturated hydrocarbon derivatives. These increments are larger than what has been observed in other instances of O/S replacement in the inner coordination shell of a metal. For example, shifts of ~0.2 V per atom are reported for metal–acetylacetonates [2,4] and oxo-bridged Mo(V) complexes [3] and of 0.10–0.12 V for $MoFe_3S_4$ dicubanes in which PhS^- has been substituted for PhO^- on the cluster exterior [5]. The present observations suggest a particularly strong interaction between the ligand donor atoms and the Mo d_{xy} electron transfer orbital of the $HB(Me_2pz)_3MoO(L\text{-}L)$ complexes. Enemark and co-workers [8b] noted that the $Mo^{V/IV}$ potential is sensitive to chelate ring size in the alkanediolate complexes (**1**) and attributed this to changes in the extent of d_π–p_π interaction between the Mo d_{xy} and ligand orbitals caused by changes in the torsional angle of the donor heteroatom. This observation suggests that overlap of the ligand donor and Mo redox orbitals may contribute to the magnitude of the observed O/S substitution effect upon $E^{\circ\prime}$.

Based on the differences in formal potential we anticipated that heterogeneous electron transfer rates would exhibit a similar dependence upon the donor atom set of the bidentate equatorial ligands. Results are illustrated in Fig. 3 where large differences in electron transfer rate constant are apparent from the differences in peak potential separation exhibited by the completely O- and completely S-substituted deriv-

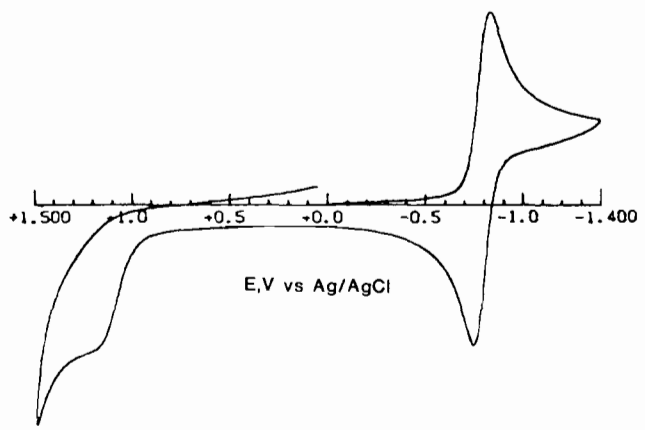

Fig. 2. Cyclic voltammetry of 1 mM $HB(Me_2pz)_3MoO(OC_2H_4S)$ in 0.3 M Bu_4NPF_6/CH_3CN; scan rate = 200 mV s^{-1}.

Table 1
Electrochemical data for reduction of $HB(Me_2pz)_3MoO(L\text{-}L)$ complexes[a]

Compound	L-L	$E^{\circ\prime}$ [b]	$i_p/\nu^{1/2}$a.c.[c]	i_{pr}/i_{pf}	D[d]
1a		−1.139	890[e]	1.1	1.7×10^{-5}
1b		−0.769	896	1.0	1.6×10^{-5}
1c		−0.339	932	0.9	1.4×10^{-5}
2a		−0.710	835	1.1	1.2×10^{-5}[g]
2b		−0.436	902	0.8	1.3×10^{-5}
2c		−0.100	741[f]	0.9	0.9×10^{-5}

[a]Recorded for 0.5–1 mM solutions of complex in 0.3 M Bu_4NPF_6/CH_3CN.

[b]Formal potential in V versus Ag/AgCl, determined as the average of cathodic and anodic peak potentials by cyclic voltammetry.

[c]Voltammetric peak current parameter in units of $\mu A\ s^{1/2}\ V^{-1/2}\ cm^{-2}\ mM^{-1}$.

[d]Diffusion coefficient in units of $cm^2\ s^{-1}$ determined by chronocoulometry.

[e]Varies with scan rate due to slow electron transfer kinetics; value reported is at 20 mV s^{-1}.

[f]Low value due to impurity.

[g]Determined by steady-state microelectrode voltammetry [11].

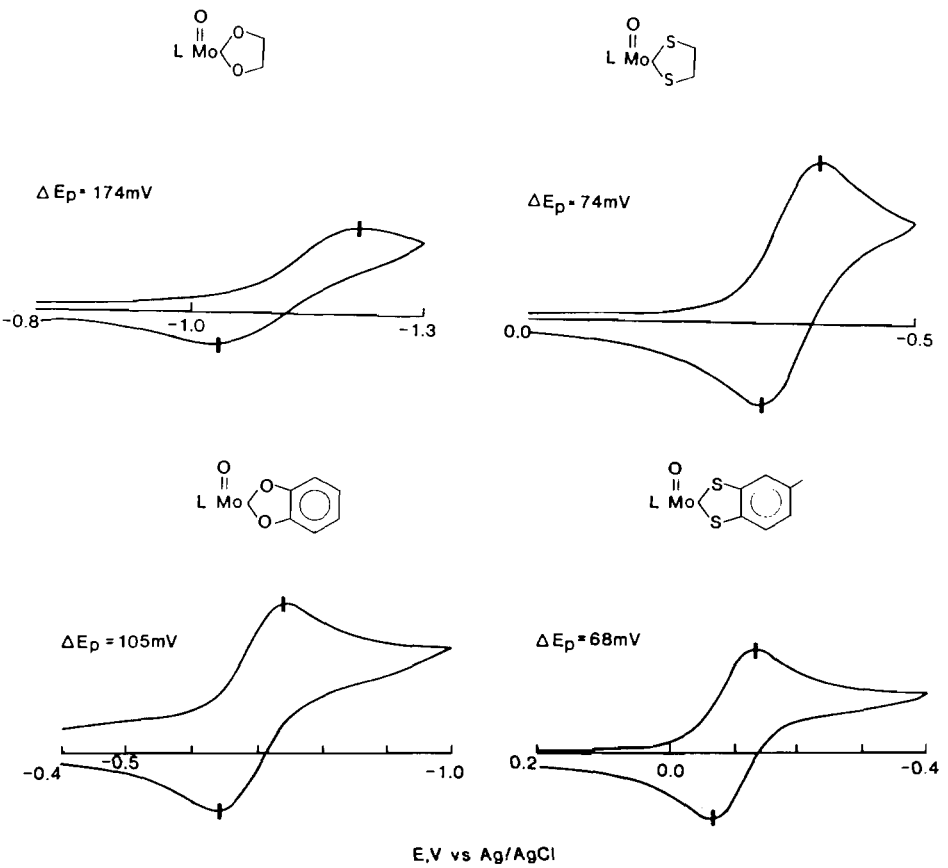

Fig. 3. Cyclic voltammetric reduction of compounds **1a**, **1c**, **2a** and **2c** at 200 mV s^{-1} in 0.3 M Bu_4NPF_6/CH_3CN.

atives. Kinetic data determined from the dependence of ΔE_p upon scan rate are presented in Table 2.

The apparent standard heterogeneous rate constants decrease as $E^{o\prime}$ becomes more negative. The effect of the electrical double layer [18] on the observed rate constants of neutral to monoanion reductions is in the same direction; thus, it is necessary to correct values of $(k_{s,h})_{app}$ in Table 2 for this contribution. The correction is applied by use of the double layer data of Fawcett and Loufty [19] obtained at Hg electrodes in CH_3CN containing 0.1 M Et_4NClO_4. The capacitance versus potential data in Ref. [19] are integrated to obtain values of q_m, the charge on the electrode surface, at each $E^{o\prime}$ assuming that the potential of zero charge is −0.192 V versus Ag/AgCl for the Pt/0.3 M $Bu_4NPF_6(CH_3CN)$ interface [20]. The outer Helmholtz plane potential, ϕ_2, is calculated from the relationship

$$\phi_2 = (2RT/F)\ \sinh^{-1}[q_m/(8RT\epsilon\epsilon_0 C^*)^{1/2}] \quad (4)$$

where C^* is the supporting electrolyte concentration (0.1 M), ϵ is the dielectric constant of acetonitrile [21] and ϵ_0 is the permittivity of free space (8.85×10^{-12} $C^2\ N^{-1}\ m^{-2}$). Values of ϕ_2 were corrected by addition of 28 mV to account for the difference in supporting electrolyte concentrations. Corrected values of $k_{s,h}$ were calculated from Eq. (5) [18]

$$(k_{s,h})_{corr} = (k_{s,h})_{app}\ \exp(-0.5\alpha F\phi_2/RT) \quad (5)$$

assuming a value of $\alpha = 0.50$ for the transfer coefficient. Results are presented in the last two columns of Table 2.

Inspection of the data in Table 2 reveals that the heteroatom donors of the L-L ligands exert a profound influence on the kinetics of $Mo^{V/IV}$ electron transfer. The corrected values of $k_{s,h}$ cover a range of approximately one and one-half orders of magnitude. Although these values of $(k_{s,h})_{corr}$ must be considered approximate by virtue of the approximate nature of the ϕ_2 calculations, the variation in rate constant is much larger than can be accounted for by uncertainties in the double layer correction. Fig. 4 contains a plot of $\log(k_{s,h})_{corr}$ versus $E^{o\prime}$ illustrating that smaller electron transfer rate constants are observed for couples with more negative redox potentials. The correlation is consistent with a previous observation (involving $Co^{III/II}$ and $Co^{II/I}$ couples of axially substituted macrocycle complexes [22]) that changes in ligand donor strength cause the kinetics and thermodynamics of metal-centered electron transfer reactions to vary in a parallel manner. Furthermore, a greater effectiveness of saturated versus aromatic hydrocarbon framework in transmitting the

Table 2
Electrode kinetic data for reduction of $HB(Me_2pz)_3MoO(L\text{-}L)$ complexes[a]

Compound	L-L	$(k_{s,h})_{app}$[b]	ϕ_2[c]	$(k_{s,h})_{corr}$[d]
1a		0.0015 ± 0.0001	−87	0.0082
1b		0.0027 ± 0.0011	−69	0.0103
1c		0.14 ± 0.04	−27	0.24
2a		0.023 ± 0.08	−65	0.081
2b		0.21 ± 0.03	−40	0.45
2c	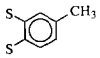	0.22 ± 0.03		0.22[e]

[a]Recorded for 0.5–1 mM solutions of complex in 0.3 M Bu_4NPF_6/CH_3CN at 23 °C at Pt electrodes.
[b]Apparent standard heterogeneous rate constant in units of cm s^{-1}.
[c]Electrical double layer potential in units of mV calculated as described in text.
[d]Corrected standard heterogeneous rate constant in units of cm s^{-1}.
[e]Uncorrected because the formal potential of this couple is close to the estimated potential of zero charge.

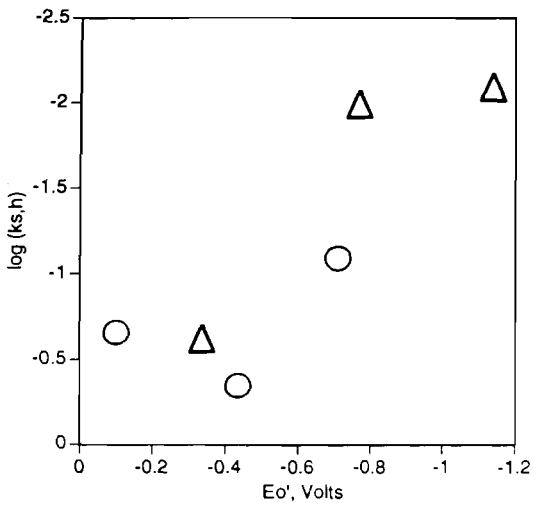

Fig. 4. Plot of $\log(k_{s,h})_{corr}$ vs. $E^{o\prime}$ for reduction of $HB(Me_2pz)_3MoO(L\text{-}L)$ complexes. Δ = saturated, O = aromatic ligands.

influence of O/S substitution to the metal center is apparent in the values of $(k_{s,h})_{corr}$ and $E^{o\prime}$.

Rationalization of these observations is provided by reference to the theory of hard and soft acids and bases [23]. Fig. 5 illustrates qualitatively the result of interaction between the ligand donor atom orbitals and the singly occupied d_{xy} orbital on Mo. This interaction results in stabilization of the metal–ligand orbitals that are involved in bond formation and destabilization of

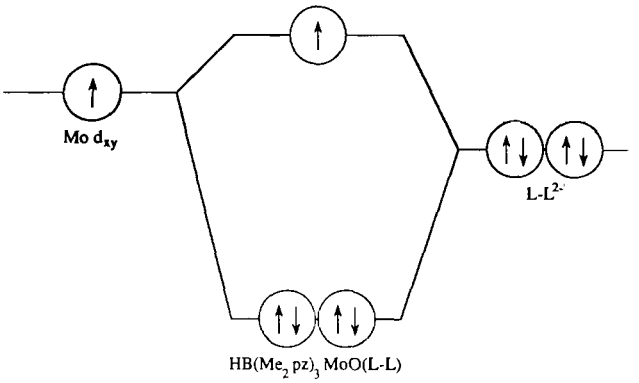

Fig. 5. Illustration of the interaction between Mo d_{xy} redox orbital and L-L donor atom orbitals in $HB(Me_2pz)_3MoO(L\text{-}L)$ complexes.

the metal-centered orbital that is involved in electron transfer. Stronger interaction leads to stronger metal–ligand bonds, whose deformations contribute to the electron transfer barriers, and to a higher energy metal-centered redox orbital, which influences $E^{o\prime}$. Thus, a correlation between reduction potential and electron transfer rate is anticipated. The $HB(Me_2pz)_3MoO^{2+}$ fragment can be viewed as a hard acid. A stronger interaction and greater splitting of orbital energies is anticipated upon interaction of this species with hard rather than soft bases. The scale of empirical hardness parameters in Ref. [23] indicates that alkoxide and phenoxide donors are harder bases than the corresponding thiolates and that saturated RO^- and RS^- donors are harder bases than their aromatic counterparts. The trends in $E^{o\prime}$ and $(k_{s,h})_{corr}$ in Tables 1 and 2 are consistent with these expectations.

Finally, it is of interest to inquire into the structural features that contribute to the differences in electron transfer rate constant between O- and S-substituted derivatives. The Marcus theory applied to electrode reactions [1c,e] defines the standard heterogeneous rate constant as

$$k_{s,h} = A \exp(-(\Delta G^*_{is} + \Delta G^*_{os})/RT) \quad (6)$$

where A is the pre-exponential factor and ΔG^*_{is} and ΔG^*_{os} are the inner- and outer-shell free energies of reorganization, respectively. If we assume that only inner-shell terms contribute to differences in rate, then the relative rate constants of O- and S-substituted derivatives can be expressed as:

$$\ln[(k_{s,h})_{Mo\text{–}S}/(k_{s,h})_{Mo\text{–}O}] = [(\Delta G^*_{is})_{Mo\text{–}O} - (\Delta G^*_{is})_{Mo\text{–}S}]/RT = \Delta(\Delta G^*_{is})/RT \quad (7)$$

By use of the corrected standard heterogeneous rate constants in Table 2 the difference in inner-shell barrier height, $\Delta(\Delta G^*_{is})$, is calculated to be 7.85 kJ mol^{-1} between compounds **1a** and **1c** and 2.45 kJ mol^{-1} between compounds **2a** and **2c**. Individual inner-shell barriers can be calculated from the relationship

$$\Delta G^{*}_{is} = \tfrac{1}{2}\sum f_i(\Delta a/2)^2 \quad (8)$$

where f_i is the force constant of the metal–ligand bond and Δa is the difference in bond lengths between the two oxidation states. Assuming vibrational frequencies [24] of 580 and 300 cm^{-1} and reduced masses of 13.7 and 24.0, force constants of 270 and 125 N m^{-1} are estimated for Mo–O and Mo–S bonds, respectively. If it is assumed that the entire difference in barrier heights results from displacement of the Mo–O and/or Mo–S bonds to the bidentate ligands, then these bond distances must change ~20 pm between the Mo^{V} and Mo^{IV} oxidation states in the case of the 1,2-disubstituted ethanes and ~10 pm in the case of the 1,2-disubstituted benzenes to produce the observed range of rate constants. Structural data are not available to test this prediction. However, bond distance changes of this magnitude would be unusual for electron transfer involving a non-bonding metal-centered redox orbital [25]. Thus, it is likely that inner-shell reorganization is shared with other bonds in the Mo coordination sphere. The molybdenum–oxo multiple bond distance does not differ significantly between the Mo^{V} and Mo^{IV} oxidation states [26]. However, examination of X-ray structural data for the $MoON_3S_2$ compounds, $HB(Me_2pz)_3Mo^{V}O(SPh)_2$ [8a], $HB(Me_2pz)_3Mo^{IV}O\{S_2P(OEt)_2\}$ [27] and $HB(Me_2pz)_3Mo^{IV}O(S_2CNPr_2)$ [28], reveals that the Mo–N bond *trans* to Mo=O is nearly 10 pm longer in the Mo^{IV} oxidation state. Changes in molybdenum-to-pyrazolyl nitrogen bond distances, therefore, may account for some of the differences in inner-shell reorganization energies. However, these changes must reflect the identity of donor atoms present at the remaining coordination sites if barrier height differences of 7.85 and 2.45 kJ mol^{-1} are to be observed between fully O- and S-substituted derivatives.

Additional factors that could contribute to the disparate rates of the O- and S-substituted complexes are differences in outer-shell activation energies and in the adiabaticities of the electrode reactions. ΔG^{*}_{os} (Eq. (6)) varies inversely as the radius of the reacting molecule. Therefore, smaller outer-shell barriers are anticipated for aromatic versus saturated ligands and for S- versus O-substituted derivatives. The observed rate constants are consistent with these trends. The presence of non-adiabatic effects in heterogeneous electron transfer reactions of diffusing reactants has not been demonstrated unequivocally, although it has been argued [29] that the slow electrochemical kinetics of the tris(hexafluoroacetylacetonato)$Ru^{III/II}$ couple are explicable on this basis as a consequence of the insulating character of the ligand's CF_3 substituents. For $HB(Me_2pz)_3Mo^{V/IV}$(L-L) redox couples, it is anticipated that greater electronic coupling with the electrode surface would occur for S-substituted derivatives because of the greater spatial extent of sulfur orbitals. Delocalization of the unpaired Mo-centered electron onto S is apparent in the EPR spectra of these compounds [8]. Differences in electron tunnelling probability, if present, would be expressed within the pre-exponential factor, A, of Eq. (6); reorganization energies are contained in the exponential term. Determination of activation parameters for $HB(Me_2pz)_3Mo^{V/IV}O$-(L-L) electrode reactions would provide an assessment of electronic and nuclear contributions to the electron transfer rate differences observed for these compounds.

Acknowledgement

Support of this research by the National Science Foundation (CHE-9214748) is gratefully acknowledged.

References

[1] (a) R.A. Marcus, *J. Chem. Phys., 24* (1956) 966; (b) N.S. Hush, *Trans. Faraday Soc., 57* (1961) 557; (c) R.A. Marcus, *Electrochim. Acta, 13* (1968) 995; (d) N. Sutin, *Prog. Inorg. Chem., 30* (1983) 441; (e) M.J. Weaver, in R.G. Compton (ed.), *Comprehensive Chemical Kinetics*, Vol. 27, Elsevier, Amsterdam, 1987, pp. 1–60; (f) R.A. Marcus, *Angew. Chem., Int. Ed. Engl., 32* (1993) 1111.
[2] (a) A.M. Bond, R.L. Martin and A.F. Masters, *Inorg. Chem., 14* (1975) 1432; (b) *J. Electroanal. Chem., 72* (1976) 187.
[3] F.A. Schultz, V.R. Ott, D.S. Rolison, D.C. Bravard, J.W. McDonald and W.E. Newton, *Inorg. Chem., 17* (1978) 1758.
[4] G.A. Heath and J.H. Leslie, *J. Chem. Soc., Dalton Trans.*, (1983) 1587.
[5] W.E. Cleland, Jr. and B.A. Averill, *Inorg. Chim. Acta, 107* (1985) 187.
[6] F.A. Schultz, *J. Electroanal. Chem., 213* (1986) 169.
[7] H.-J. Küppers, A. Neves, C. Pomp, D. Ventur, K. Wieghardt, B. Nuber and J. Weiss, *Inorg. Chem., 25* (1986) 2400.
[8] (a) W.E. Cleland, Jr., K.M. Barnhart, K. Yamanouchi, D. Collison, F.E. Mabbs, R.B. Ortega and J.H. Enermak, *Inorg. Chem., 26* (1987) 1017; (b) C.-S.J. Chang, D. Collison, F.E. Mabbs and J.H. Enemark, *Inorg. Chem., 29* (1990) 2261; (c) C.-S.J. Chang and J.H. Enemark, *Inorg. Chem., 30* (1991) 683.
[9] S. Trofimenko, *Inorg. Chem., 10* (1971) 504.
[10] A. Fitch and D.H. Evans, *J. Electroanal. Chem., 202* (1986) 83.
[11] X.H. Mu and F.A. Schultz, *Electroanalysis, 2* (1990) 353.
[12] R.R. Gagné, C.A. Koval and G.C. Lisensky, *Inorg. Chem., 19* (1980) 2855.
[13] R.S. Nicholson, *Anal. Chem., 37* (1965) 1351.
[14] W.J. Bowyer, E.E. Engelman and D.H. Evans, *J. Electroanal. Chem., 262* (1989) 67.
[15] J. Heinze, *Ber. Bunsenges. Phys. Chem., 85* (1981) 1096.
[16] (a) M.I. Montenegro and D. Pletcher, *J. Electroanal. Chem., 200* (1986) 371; (b) D.O. Wipf, E.W. Kristensen, D.R. Deakin and R.M. Wightman, *Anal. Chem., 60* (1988) 306; (c) Z.J. Karpinski and R.A. Osteryoung, *J. Electroanal. Chem., 349* (1993) 285.
[17] J.R. Bradbury and F.A. Schultz, *Inorg. Chem., 25* (1986) 4408.

[18] P. Delahay, *Double Layer and Electrode Kinetics,* Wiley-Interscience, New York, 1965.
[19] W.R. Fawcett and R.O. Loutfy, *Can. J. Chem., 51* (1973) 230.
[20] S. Sahami and M.J. Weaver, *J. Electroanal. Chem., 124* (1981) 35.
[21] J.A. Riddick, W.A. Bunger and T.K. Sakano, *Organic Solvents: Physical Properties and Methods of Purification,* Wiley, New York, 4th edn., 1986.
[22] D. Faure, D. Lexa and J.-M. Savéant, *J. Electroanal. Chem., 140* (1982) 285, 297.
[23] R.G. Pearson, *Coord. Chem. Rev., 100* (1990) 403.
[24] K. Nakamoto, *Infrared and Raman Spectra of Inorganic and Coordination Compounds,* Wiley, New York, 4th edn., 1986.
[25] D.J. Szalda, C. Creutz, D. Mahajan and N. Sutin, *Inorg. Chem., 22* (1983) 2372.
[26] J.M. Mayer, *Inorg. Chem., 27* (1988) 3899.
[27] S.A. Roberts, C.G. Young, W.E. Cleland, Jr., R.B. Ortega and J.H. Enemark, *Inorg. Chem., 27* (1988) 3044.
[28] N.E. Heimer and W.E. Cleland, Jr., *Acta Crystallogr., Sect. C, 47* (1991) 56.
[29] M.J. Weaver, D.K. Phelps, R.M. Nielson, M.N. Golovina and G.E. McManis, *J. Phys. Chem., 94* (1990) 2949.